A Different Perspective on Critically Stressed Fractures and Their Impact on Fluid Flow*

Kevin Bisdom[1], Giovanni Bertotti[1], and Hamidreza M. Nick[1,2]

Search and Discovery Article #41877 (2016)**
Posted September 19, 2016

*Adapted from extended abstract prepared in relation to a poster presentation given at AAPG 2016 Annual Convention and Exhibition, Calgary, Alberta, Canada, June 16-22, 2016

[1]Geoscience & Engineering, Delft University of Technology, Delft, Netherlands (k.bisdom@tudelft.nl)
[2]Technical University of Denmark, The Danish Hydrocarbon Research and Technology Centre, Copenhagen, Denmark

Introduction

Naturally fractured reservoirs are often characterized by high-density multi-scale fracture networks, organized in multiple orientation families. However, not all fractures contribute to fluid flow under in-situ stress conditions. The Coulomb friction criterion has long been applied to predict the probability of reactivating faults and fractures in the subsurface, and hence quantify which part of the fracture network contributes to flow at in-situ stress conditions (Barton et al., 1995; Rogers, 2003).

Coulomb friction predicts that only the fractures that are sub-parallel to the maximum horizontal stress are reactivated. However, in both outcrops and reservoirs, it is commonly found that multiple orientation families, often organized in orthogonal patterns, are at least partially open. Partial cementation of fractures may explain how fractures can be open even when they do not meet the Coulomb criterion, as cement often forms bridges that prevent the fracture from fully closing (Laubach et al., 2004). However, in the absence of these cement bridges, roughness of the fracture surface itself, combined with minor amounts of shearing during opening, provides an additional explanation for the occurrence of hydraulically open fractures. The Barton-Bandis model, based on experimental work on outcropping rocks, quantifies the aperture that may remain when irregular fracture walls no longer perfectly interlock (Barton and Bandis, 1980; Bandis et al., 1983; Olsson and Barton, 2001; Barton, 2014).

We implement the Barton-Bandis aperture model into a Finite Element code to model the aperture distribution at in-situ stress conditions for natural fracture network geometries with varying degrees of complexity and intensity, digitized from outcropping pavements. The Barton-Bandis method has been implemented into other numerical modeling codes, but the application is often limited to single-fracture models or synthetic fracture networks. Our approach allows for modeling aperture in complex fracture networks, with a coupling to flow modeling, enabling us to quantify the impact of aperture variations on permeability. We use this approach to compare the aperture and permeability modeled by the Barton-Bandis approach with the more commonly used Mohr-Coulomb method, to quantify the implications of the aperture

model used on permeability. The absolute apertures for the Mohr-Coulomb method are calculated using the linear length-aperture scaling model (Atkinson, 1984).

Methodology: From Outcropping Fractures to Aperture and Flow

Fracture Data Acquisition

Modeling fluid flow patterns in naturally fractured reservoirs require an accurate description of the network geometry. Characterizing the network geometry in subsurface reservoirs is challenging, as the only direct measurements of orientation and spacing are obtained from well data, which provide a 1-D view of a complex 3-D system. Furthermore, well fracture data suffers from sampling artifacts, and correction methods for these artifacts only work for small corrections (Bisdom et al., 2014).

The extrapolation of 1-D well data to a 2-D or 3-D network is commonly done using stochastic modeling approaches (Dershowitz et al., 2000). The resulting Discrete Fracture Networks may honor the limited well data, but the stochastic patterns do not capture the natural variability that is observed in outcropping analogs (Bisdom et al., 2014). Therefore, outcropping analogs are used to better understand fracture geometry and, by using the outcrops as input for flow models, to understand the fluid flow patterns.

Scanlines and laser scanning tools are common methods to digitize outcropping fracture networks (Mauldon and Mauldon, 1997; Wilson et al., 2011; Hodgetts, 2013). Although measuring fractures along scanlines is the most commonly used method, it only provides spacing and orientation of a small subset of the network, which is similar to the data obtained from wells in the subsurface. On the other hand, laser scanning digitizes the entire outcrop and, merged with outcrop photographs, provides a high-resolution 3-D outcrop model, in which the entire fracture network can be digitized in 2-D or 3-D. However, the method is inflexible, as it requires relatively bulky equipment and requires significant processing before a usable fracture dataset can be extracted.

Instead, we use a fast method to digitize entire outcrops, by using a drone, equipped with GPS and a camera. The drone photographs outcrops with any orientation, including pavements or dipping surfaces. Using photogrammetry, combined with GPS data, the images are processed into 3-D models, which have a slightly decreased resolution compared to laser scanning, but processing and interpretation of photogrammetry models is several times faster (Figure 1) (Bond et al., 2015). With this approach, we can process the acquired data into models within hours, and using interpretation tools, such as OpenPlot and DigiFract, fracture data is rapidly extracted (Hardebol and Bertotti, 2013; Tavani et al., 2014).

Using the workflow with the drone and photogrammetry, we have collected a unique database with over 13,000 fractures digitized from a range of outcropping pavements in Tunisia and Brazil. These models cover areas of up to 500x500m, with a resolution high enough to capture length scales from less than a meter to several hundred meters. The large extent and high resolution ensure that the datasets suffer from a minimum of censoring and truncation artifacts (Bonnet et al., 2001).

Mechanical Modeling of Stress and Aperture

We use these unique fracture patterns, which capture the intrinsic heterogeneity not captured by stochastic models, as a basis for mechanical and fluid flow modeling. Key to our approach is that we keep the multiscale digitized patterns as discrete features in the entire workflow, without any upscaling. This allows us to model flow through the entire network, identifying which fractures contribute to fluid flow. To model flow through the discrete fractures, aperture needs to be defined. Aperture measurements in outcrops are, however, not representative, as these have been changed during exhumation. Only outcropping veins may be representative, if these veins have been formed during burial. We, therefore, use mechanical models to quantify aperture, where the relation between local stress and aperture is quantified, using the empirical Barton-Bandis approach.

The Barton-Bandis model assumes that fracture surfaces are not planar, but irregular with a given roughness (Barton and Choubey, 1977). Even if pore pressure is lower than the normal stress acting on the fracture surface, the fracture can remain open because of a combination of shear displacement and poorly interlocking fracture walls (Figure 2). This model explains how fractures can be conduits for flow even if they are not critically stressed as defined by Mohr-Coulomb (Olsson and Barton, 2001). Barton-Bandis distinguishes between physical or normal aperture, which is the actual opening between two fracture surfaces and hydraulic aperture, which is the aperture that effectively controls flow (Barton, 2014; Lei et al., 2014). The hydraulic aperture is equal to or smaller than the physical aperture. The exact relation between the two apertures is dependent on the amount of shear displacement that the fracture experiences, compared to a fixed peak shear displacement that depends only on the fracture geometry (Barton and Bandis, 1980; Bandis et al., 1983). Both apertures depend differently on orientation and applied stress.

To use the Barton-Bandis method, the local shear and normal stresses acting on a fracture surface need to be known. Mohr circles provide an approximation of these stresses, based principally on the orientation of the fracture and far-field stresses (Zoback, 2007). However, in complex fracture networks, the arrangement of nearby fractures is found to create stress perturbations, such that local stress is different from the far-field stresses. To model the local stresses in the digitized fracture networks, we use Finite Element modeling. The models are constructed using ABAQUS (Dassault Systemes), where we add our own functionality to represent the digitized fracture network as explicit discontinuities ('seams') that influence the stress distribution (Figure 3). Along each fracture surface, local and shear stress vary, resulting in a heterogeneous aperture distribution along single fractures (Figure 4 and Figure 5a,b).

Equivalent Permeability Modeling

The resulting aperture model contains closed segments that can act as flow bottlenecks. To quantify the impact of a heterogeneous aperture distribution on fluid flow, we model equivalent permeability, which represents the permeability of the matrix and fractures combined. The equivalent permeability is calculated utilizing a Finite-Element Finite-Volume (FEFV) approach in which the steady state continuity equation for flow $\nabla \cdot q = 0$ is solved, where q is the Darcy velocity $q = -k \nabla p / \mu$ (in m/s), with pressure p in Pa, viscosity μ in Pa s and intrinsic permeability k in m^2 (Matthäi et al., 2007). This approach uses the exact same meshed fracture network from the mechanical models. The rock matrix is represented by 2-D triangular elements, and the fractures are 1-D line elements. Each fracture node has an aperture calculated from the mechanical model. This approach is implemented into the Complex System Modeling Platform (CSMP++) (Paluszny and Matthäi, 2010; Nick and Matthäi, 2011). We apply a pressure gradient of 10 kPa in both horizontal directions of rectangular 2-D models. By integrating the fluid

flux at the model boundaries we derive the equivalent permeability through Darcy flow (Matthäi and Nick, 2009). The equivalent permeability thus represents the combined fracture-matrix flow of the model (Figure 5c,d).

Dataset: Large-scale Fracturing in the Potiguar Basin, NE Brazil

We apply the integrated workflow from fracture data acquisition to aperture and flow modeling to outcropping pavements of the Jandaíra Formation in the Potiguar Basin (NE Brazil) (Maia and Bezerra, 2015). The Jandaíra, an Upper Cretaceous carbonate formation with a relatively simple burial history, is intensely fractured (Figures 6 and 7). The formation crops out in large parts of the basin, providing large sub-horizontal pavements in which fractures can be studied quantitatively, with a minimum of censoring and truncation artifacts. Using the drone, we digitize a series of pavements that contain bed-perpendicular fracture networks with a range of orientations and topological relations, providing complex deterministic fracture patterns that form a basis for the aperture and flow models. Although fracture patterns in most outcrops follow power-law size scaling relations, the fracture arrangements are highly varying. We focus on one pavement to quantify the aperture and permeability resulting from the Barton-Bandis model compared to the Mohr-Coulomb model (Figure 8). The aperture and permeability in the other pavements, as well as the relation between geometry, aperture and permeability, has been quantified in earlier work (Bisdom et al., 2016).

For the Barton-Bandis and Mohr-Coulomb models, we use the same identical fracture network geometry, with the same far-field stress, elastic rheology and boundary conditions. The outcrop consists of 791 fractures with a scattered orientation distribution and a complex topology. Two sets of long fractures are identified, striking approximately NNW-SSE and WNW-ESE, with smaller fractures showing a wide range of orientations abutting these larger systems. The average P21 intensity is $0.29m^{-1}$, with an average length of 5.8m and a connectivity of 0.083 intersections per m^2. This network is converted into a 2-D mechanical and flow mesh, consisting of approximately 320,000 triangular elements. A horizontal maximum stress of 30MPa (Shmax) is applied in the N-S direction, resulting in a Poisson's stress of 10MPa in the E-W direction, based on a Poisson's ratio of 0.3 for the rock matrix. The matrix is fully elastic with a homogeneous rock density of 2300 kg/m^3 and a Young's Modulus of 40GPa. Matrix permeability is 10mD, with a porosity of 20%.

For the Barton-Bandis model, we calculate first the physical aperture as a function of normal stress, followed by the hydraulic aperture, which is a function of shear stress. For Mohr-Coulomb, we first define physical aperture using the sub-critical crack growth model, which predicts that aperture scales linearly with fracture length, and then use Mohr-Coulomb to define which physical apertures are also hydraulically open.

Results

The critically stressed hydraulic aperture distribution for the Mohr-Coulomb model predicts that 50% of the network is hydraulically open, with apertures of up to 40mm. In the Barton-Bandis model, more than 80% of the network is critically stressed, with a maximum aperture of 0.21mm (Figure 8a,c). The average apertures are closer to each other, although Barton-Bandis aperture is still 25 times smaller, with an average of 0.19mm in the Barton-Bandis model and 5mm in the Mohr-Coulomb model.

Although the average aperture of Mohr-Coulomb is much higher, 30% more fractures are hydraulically closed in this model compared to Barton-Bandis. In both models, the orientation of a fracture with respect to the direction of Shmax is the main controlling factor that defines whether a fracture is critically stressed. However, Mohr-Coulomb does not distinguish between small or large fractures, or the impact of nearby fractures on stress, while Barton-Bandis predicts that smaller fractures with more intersecting fractures have a higher probability of becoming critically stressed. Because the studied network contains many small fractures with a high connectivity, a large fraction of the network is critically stressed.

The difference in equivalent permeability in both models is relatively small (Figure 8b,d). The pressure contour lines illustrate that flow in the Mohr-Coulomb aperture model is mainly controlled by a few long fractures with large apertures, whereas the more evenly spaced contour lines in the Barton-Bandis model indicate that the increase in permeability resulting from the fractures is the cumulative effect of many small open fractures (Figure 8b,d). For a 10mD matrix permeability, a network with 50% of fractures hydraulically closed but with a high average aperture has a similar impact on flow as a network with a small average aperture but with 80% of the fractures critically stressed.

For a higher matrix permeability, the Mohr-Coulomb model has a higher permeability than the Barton-Bandis model (Figure 9). The permeability models are equal for a matrix permeability of 30mD, but the relative impact of the Barton-Bandis model on matrix flow decreases rapidly for increasing matrix permeability, while the impact of the Mohr-Coulomb model remains approximately constant, even for high matrix permeabilities. For matrix permeabilities below 10mD, the Barton-Bandis model predicts a higher increase in flow resulting from fractures compared to Mohr-Coulomb. The difference is explained by connectivity, as in a low permeability matrix, a well connected fracture network with small apertures has a bigger impact on flow than a disconnected network of fractures with large apertures. When matrix permeability is high, fractures do not need to be connected to a percolating network to impact flow, and hence large apertures are more important.

Conclusions

By integrating quantitative fracture data acquisition with a mechanical and flow modeling approach where the entire network is represented discretely, we can study the impact of aperture on fluid flow. Aperture is not measured, as outcropping apertures are not representative of flow, but modeled based on Mohr-Coulomb and Barton-Bandis stress-aperture relations. A comparison of the two methods shows that:

- In either case, the aperture distributions are heterogeneous, with partial opening and closing even along a single fracture.
- For Mohr-Coulomb, aperture depends mainly on fracture orientation, while for Barton-Bandis, length and spacing also have an impact on aperture.
- The fraction of reactivated fractures in the Barton-Bandis model is on average 80%, versus 50% based on the Coulomb criterion.
- The average aperture predicted by Barton-Bandis is 0.2mm, but especially in a low-permeable matrix, i.e., less than 25 mD, the impact of fractures on flow is significant because of the high fraction of open fractures.
- In a higher-permeability matrix, fractures that are disconnected from the main network can still contribute to flow through the matrix, so large absolute apertures have a larger impact on permeability than fracture connectivity.

Acknowledgements

We thank TOTAL SA for financial support and permission for publication. We specifically thank B. Gauthier, A. Kamp and Y. Leroy from TOTAL SA for their input. The outcropping fracture networks have been acquired and interpreted with support from F. H. Bezerra (UFRN, Brazil), S. Bouaziz, and A. Hammami (ENIS, Tunisia), H. Boro, M. van Eijk, K. Ewondo, J. van der Vaart, R. Vaughan and E. van der Voet (VU University Amsterdam, Netherlands) and K. Althuis (TU Delft, Netherlands). N.J. Hardebol is thanked for supplying DigiFract software and for productive discussions regarding the aperture models.

References Cited

Atkinson, B.K., 1984, Subcritical crack growth in geological materials: Journal of Geophysical Research, v. 89/B6, p. 4077.

Bandis, S.C., A.C. Lumsden, and N.R. Barton, 1983, Fundamentals of rock joint deformation (abstract): International Journal of Rock Mechanics and Mining Sciences & Geomechanic Abstracts, v. 20/, p. 249–268.

Barton, N., 2014, Non-linear behaviour for naturally fractured carbonates and frac-stimulated gas-shales: First Break, v. 32/2031, p. 51–66.

Barton, N., and S. Bandis, 1980, Some effects of scale on the shear strength of joints (abstract): International Journal of Rock Mechanics and Mining Sciences & Geomechanics Abstracts: p. 69–73.

Barton, N., and V. Choubey, 1977, The shear strength of rock joints in theory and practice: Rock Mechanics Felsmechanik Mecanique des Roches, v. 10/1-2, p. 1–54.

Barton, C.A., M.D. Zoback, and D. Moos, 1995, Fluid flow along potentially active faults in crystalline rock: Geology, v. 23/8, p. 683.

Bisdom, K., B.D.M. Gauthier, G. Bertotti, and N.J. Hardebol, 2014, Calibrating discrete fracture-network models with a carbonate three-dimensional outcrop fracture network: Implications for naturally fractured reservoir modeling: AAPG Bulletin, v. 98/7, p. 1351–137.

Bisdom, K., G. Bertotti, and H.M. Nick, 2016, The impact of in-situ stress and outcrop-based fracture geometry on hydraulic aperture and upscaled permeability in fractured reservoirs: Tectonophysics, 8 April. Website accessed August 29, 2016, http://www.sciencedirect.com/science/article/pii/S0040195116300531.

Bond, C. E., J.R. Shackleton, and T. Wild, 2015, From field fractures to reservoir prediction: Utilizing drones, virtual outcrop and digital data Analysis to input into discrete fracture network (DFN) mdels (abstract): AAPG Annual Convention and Exhibition, Search and Discovery Article #90216 (2015). Website accessed August 29, 2016, http://www.searchanddiscovery.com/abstracts/html/2015/90216ace/abstracts/2099690.html

Bonnet, E., O. Bour, N.E. Odling, P. Davy, I. Main, P. Cowie, and B. Berkowitz, 2001, Scaling of fracture systems in geological media: Reviews of Geophysics, v. 39/3, p. 347.

Dershowitz, B., P. LaPointe, T. Eiben, and L. Wei, 2000, Integration of discrete feature network methods with conventional simulator aitzpproaches: SPE Reservoir Evaluation & Engineering, v. 3/2, p. 165-170.

Hardebol, N.J., and G. Bertotti, 2013, DigiFract: A software and data model implementation for flexible acquisition and processing of fracture data from outcrops: Computers & Geosciences, v. 54, p. 326–336.

Hodgetts, D., 2013, Laser scanning and digital outcrop geology in the petroleum industry: A review: Marine and Petroleum Geology, v. 46, p. 335–354.

Laubach, S.E., J.E. Olson, and J.F. Gale, 2004, Are open fractures necessarily aligned with maximum horizontal stress?: Earth and Planetary Science Letters, v. 222/1, p. 191–195.

Lei, Q., J.-P. Latham, J. Xiang, C.-F. Tsang, P. Lang, and L. Guo, 2014, Effects of geomechanical changes on the validity of a discrete fracture network representation of a realistic two-dimensional fractured rock: International Journal of Rock Mechanics and Mining Sciences, v. 70, p. 507–523.

Maia, R.P., and F.H R. Bezerra, 2015, Potiguar Basin: Diversity of landscapes in the Brazilian equatorial margin, *in* B.C. Vieira, A.A.R. Salgado, and L.J.C. Santos, eds., Landscapes and Landforms of Brazil: World Geomorphological Landscapes, Dordrecht, Springer Netherlands, p. 147-157.

Matthäi, S., A. Mezentsev, and M. Belayneh, 2007, Finite Element—Node-Centered Finite-Volume Two-Phase-Flow Experiments With Fractured Rock Represented by Unstructured Hybrid-Element Meshes.

Matthäi, S.K., and H.M. Nick, 2009, Upscaling two-phase flow in naturally fractured reservoirs: AAPG Bulletin, v. 93/11, p. 1621–1632.

Mauldon, M., and J.G. Mauldon, 1997, Fracture sampling on a cylinder: From scanlines to boreholes and tunnels: Rock Mechanics and Rock Engineering, v. 303, p. 129–144.

Nick, H.M., and S.K. Matthäi, 2011, Comparison of three FE-FV numerical schemes for single- and two-phase flow simulation of fractured porous media: Transport in Porous Media, v. 90/2, p. 421–444.

Olsson, R., and N. Barton, 2001, An improved model for hydromechanical coupling during shearing of rock joints: International Journal of Rock Mechanics and Mining Sciences, v. 38/3, p. 317–329.

Paluszny, A., and S.K. Matthäi, 2010, Impact of fracture development on the effective permeability of porous rocks as determined by 2-D discrete fracture growth modeling: Journal of Geophysical Research, v. 115/B2, p. B02203.

Rogers, S.F., 2003, Critical stress-related permeability in fractured rocks: Geological Society, London, Special Publications, v. 209/1, p. 7–16.

Tavani, S., P. Granado, A. Corradetti, M. Girundo, A. Iannace, P. Arbués, J.A. Muñoz, and S. Mazzoli, 2014, Building a virtual outcrop, extracting geological information from it, and sharing the results in Google Earth via OpenPlot and Photoscan: An example from the Khaviz Anticline (Iran): Computers & Geosciences, v. 63, p. 44–53.

Wilson, C.E., A. Aydin, M. Karimi-Fard, L.J. Durlofsky, S. Amir, E.E. Brodsky, O. Kreylos, and L.H. Kellogg, 2011, From outcrop to flow simulation: Constructing discrete fracture models from a LIDAR survey: AAPG Bulletin, v. 95/11, p. 1883–1905.

Zoback, M.D., 2007, Reservoir Geomechanics: Cambridge University Press, 449p.

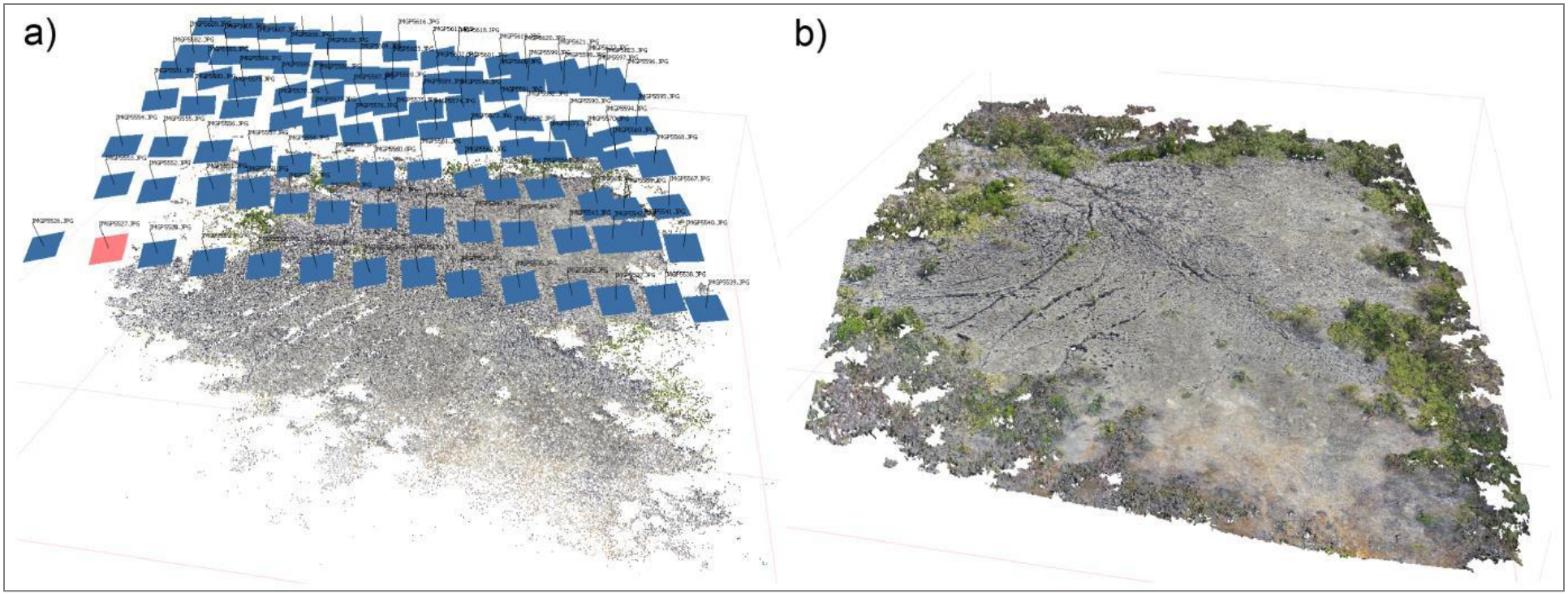

Figure 1. Processing of a grid of photographs taken by the drone, combined with GPS measurements, to generate a 3-D high-resolution georeferenced model of a fractured pavement.

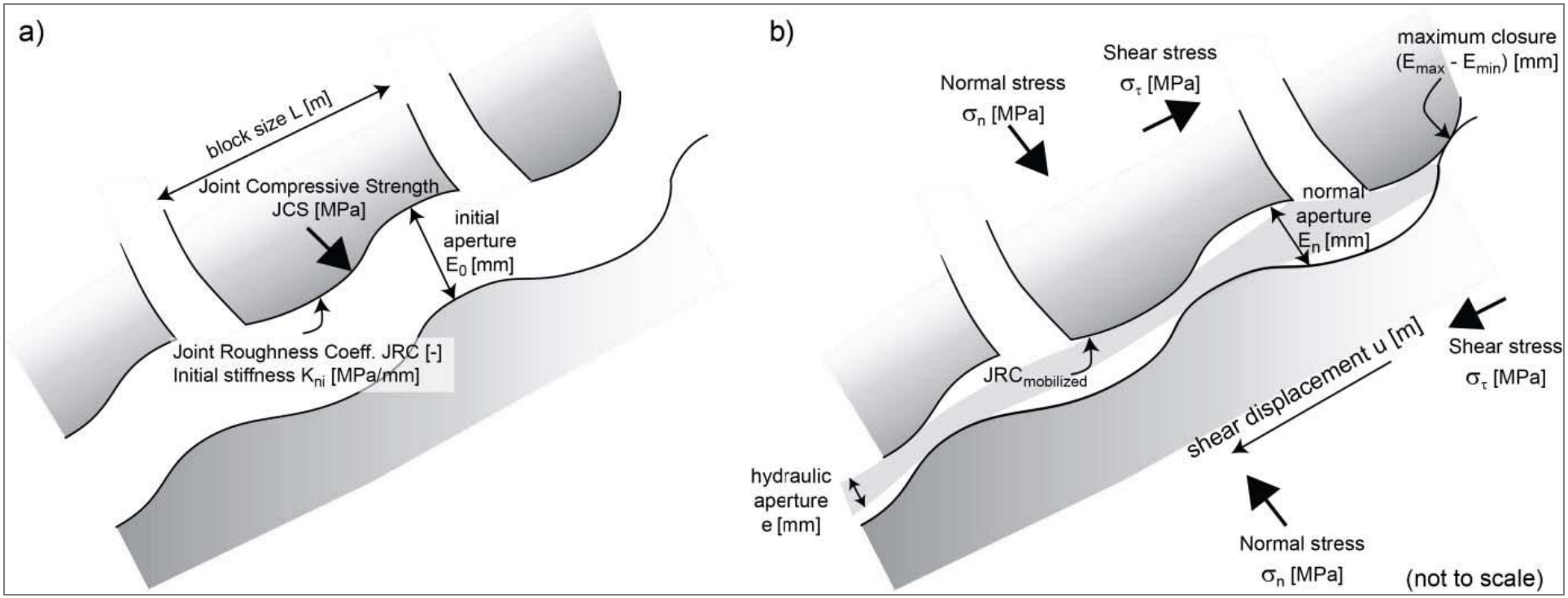

Figure 2. Visual representation of the Barton-Bandis model, which assumes that an aperture remains when irregular fracture surfaces with shear displacement no longer perfectly interlock.

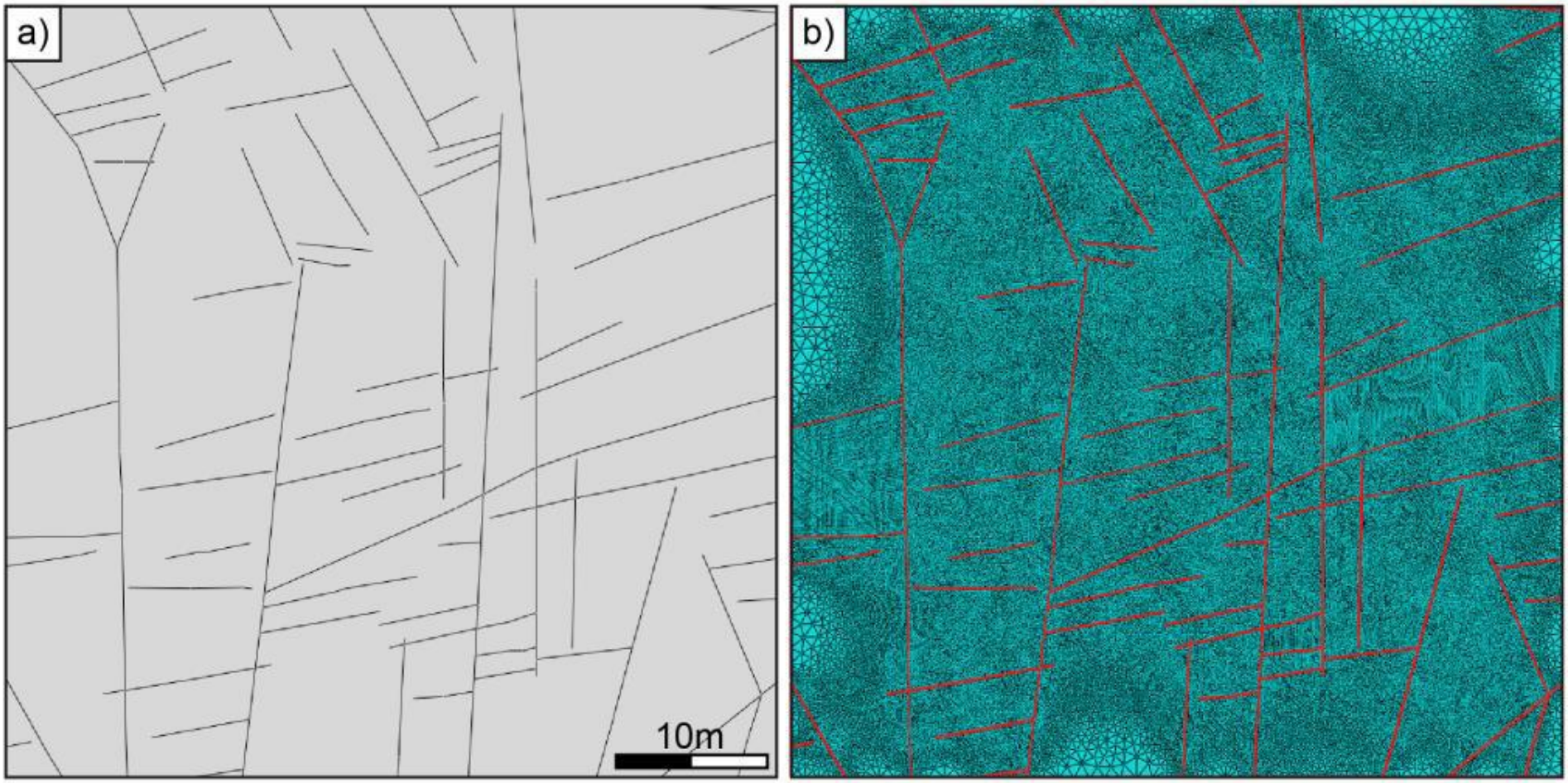

Figure 3. Conversion from a fracture geometry, digitized from an outcrop, into a fractured mesh, constructed from unstructured triangular elements.

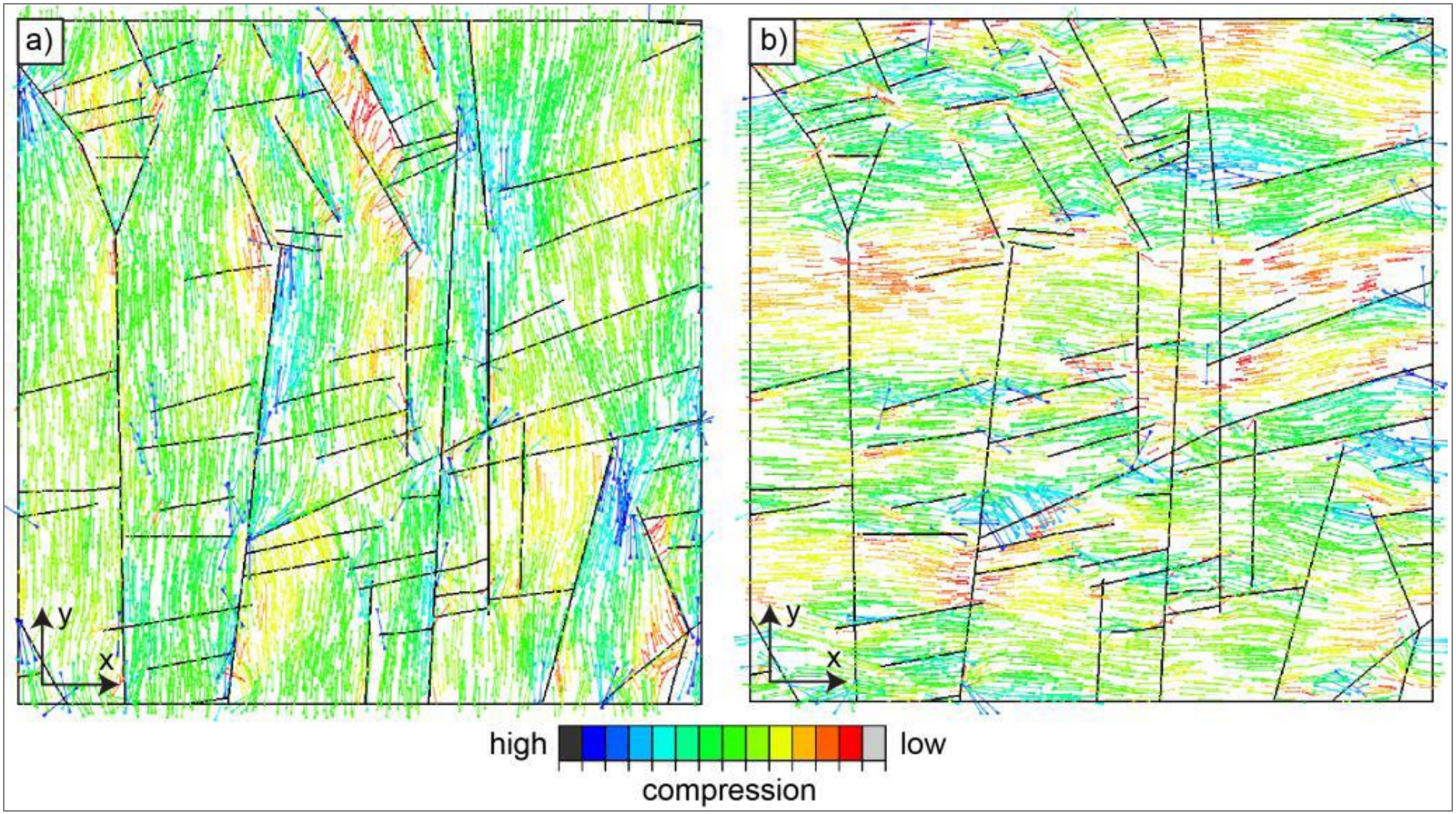

Figure 4. Local maximum (compressive) stress modeled around a fracture network, assuming a far-field maximum stress applied in the y-direction (a) and in the x-direction (b). The color and size of the arrows indicate the magnitude, whereas the direction of maximum stress is indicated by the direction of the arrows.

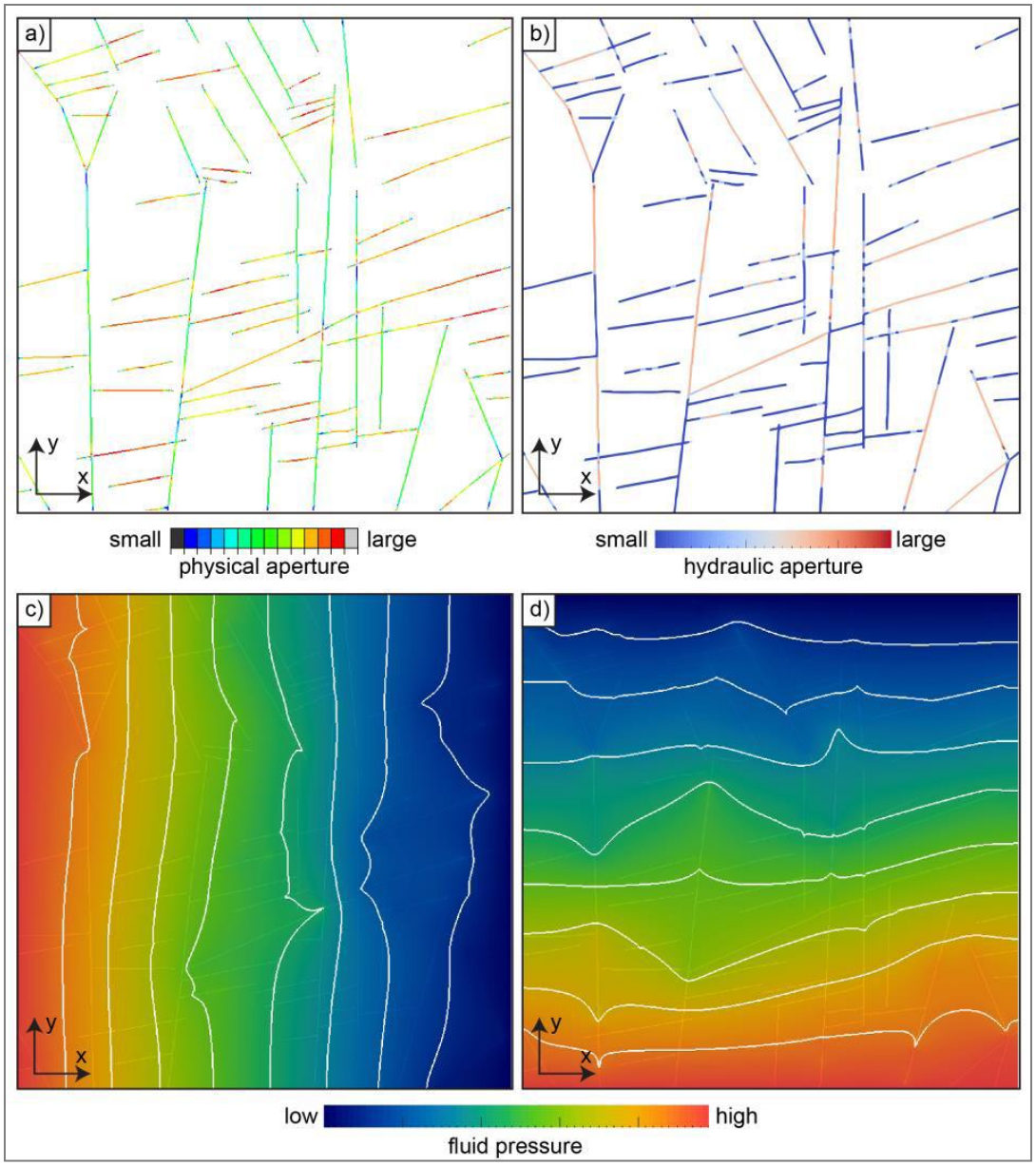

Figure 5. Physical and hydraulic aperture distributions for the fracture network and modeled stress distribution (y-direction) from the previous figure, as defined by the Barton-Bandis model. The fluid pressure distribution in x- and y-directions (c and d) are shown for the hydraulic aperture distribution in (b). The white lines indicate pressure contour lines, where large perturbations in the contours correspond to large apertures in the hydraulic aperture model.

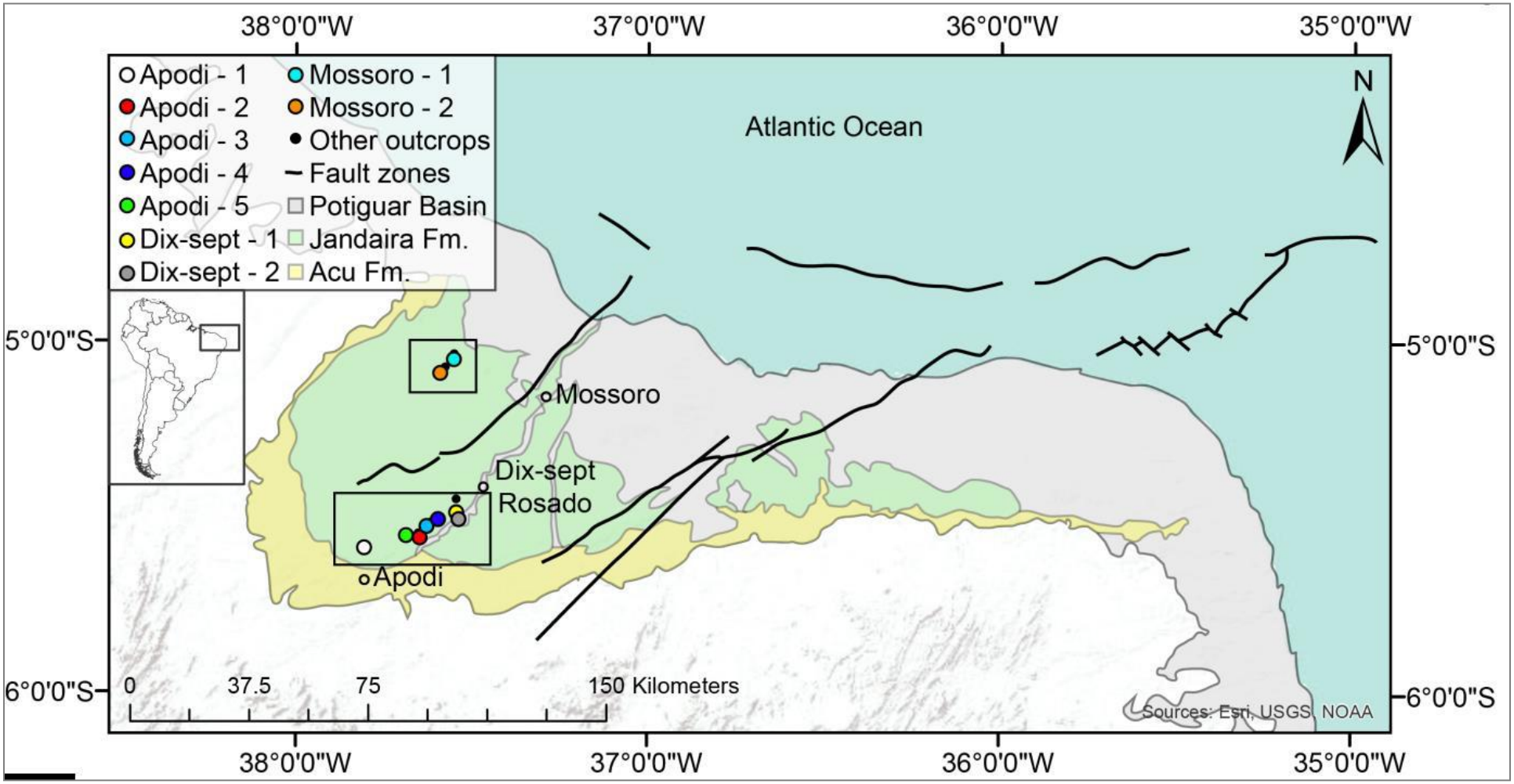

Figure 6. Overview of the onshore part of the Potiguar Basin in NE Brazil, with the locations of the digitized pavements in the basin, far from large-scale faults.

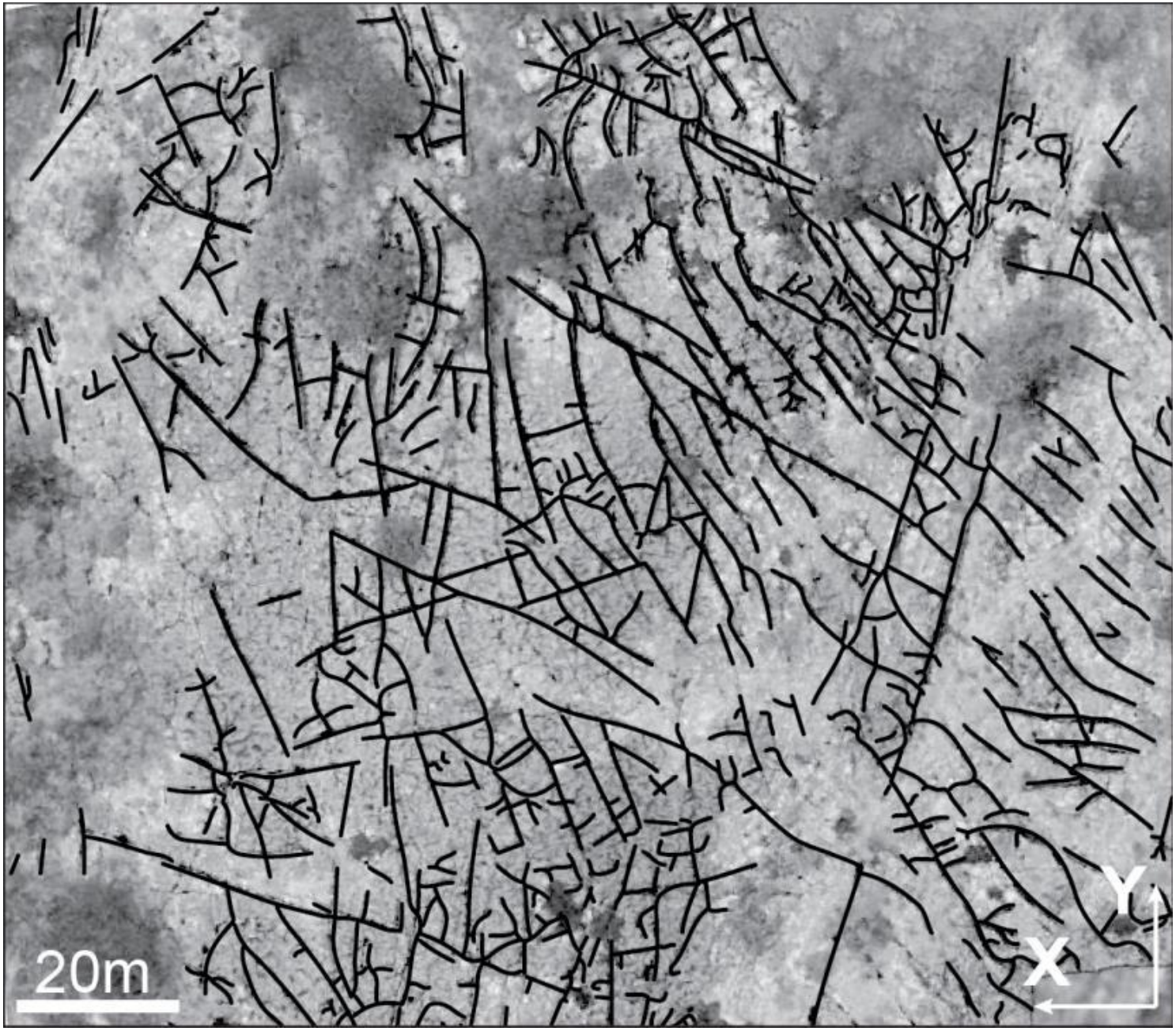

Figure 7. Backdrop image of part of an outcropping pavement of the Jandaíra Formation, with the digitized fracture network geometry used for aperture and flow modeling. North is up (in the y-direction).

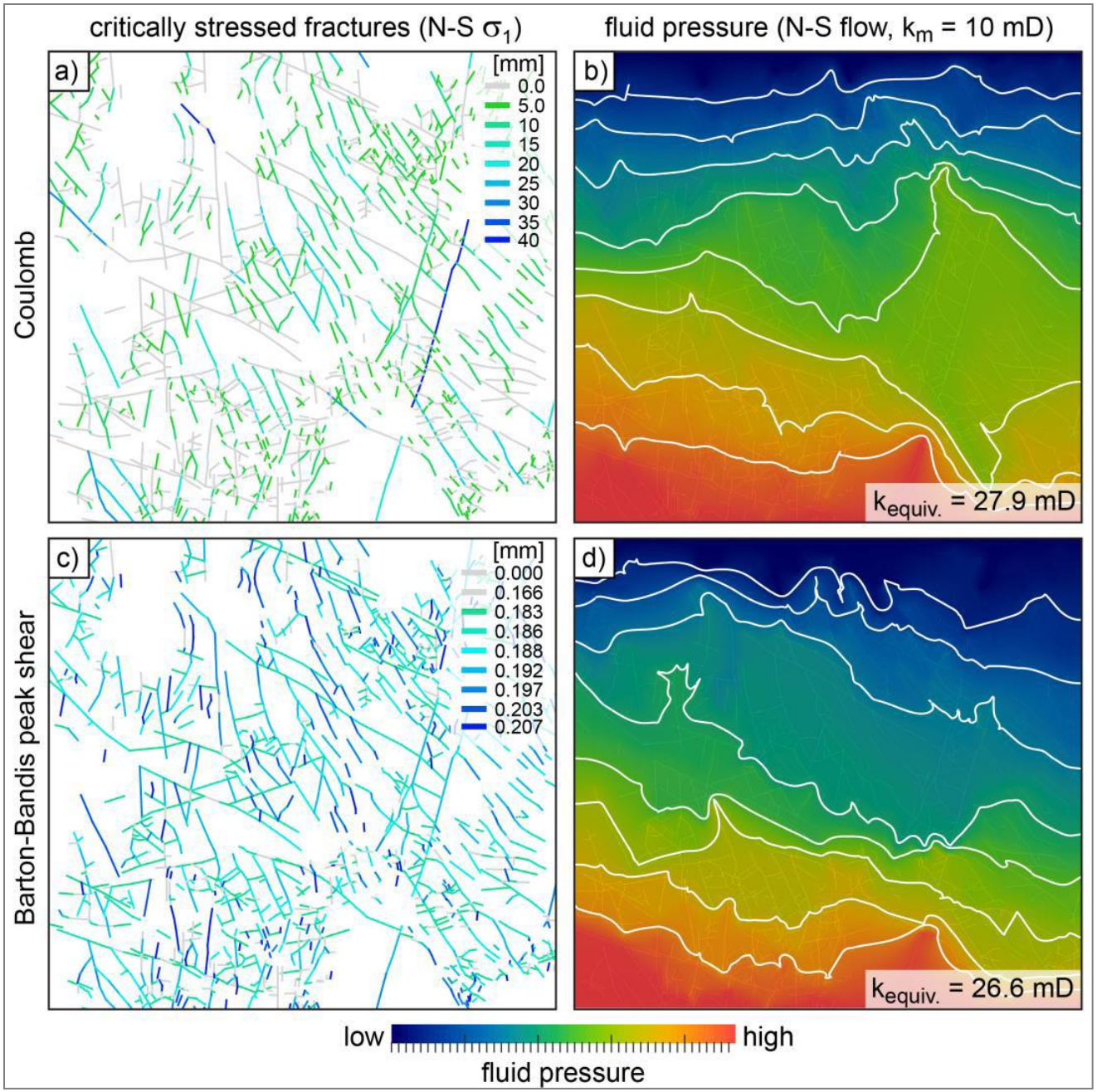

Figure 8. Critically stressed aperture distributions resulting from the Mohr-Coulomb and Barton-Bandis models (a,c),with their corresponding fluid pressure distributions assuming a N-S fluid pressure gradient (b,d). The white contour lines are pressure contours.

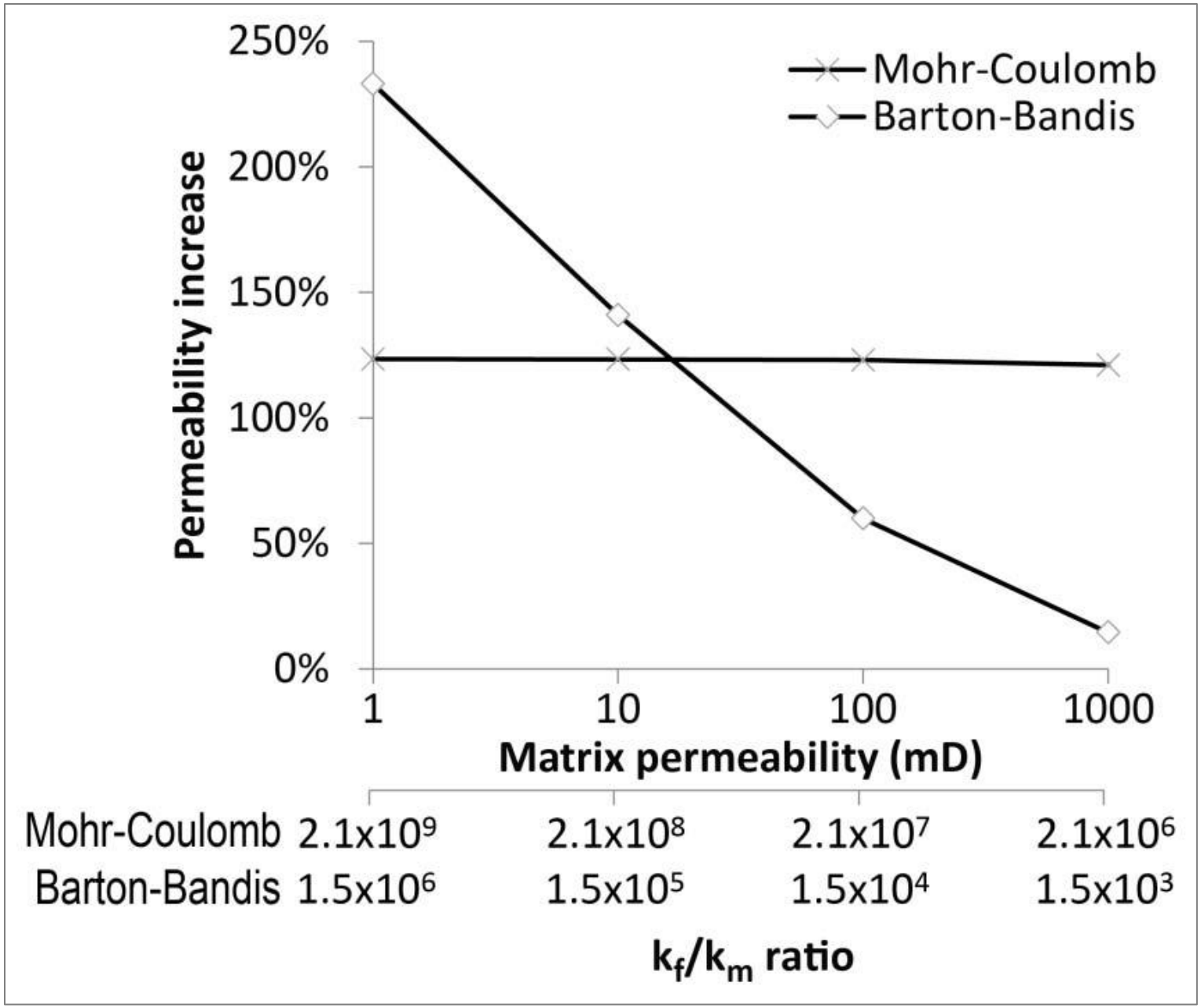

Figure 9. Increase in equivalent permeability (with respect to matrix) resulting from fractures for a range of matrix permeabilities.